

UNCLASSIFIED

AD NUMBER

AD835398

LIMITATION CHANGES

TO:

Approved for public release; distribution is unlimited.

FROM:

Distribution authorized to U.S. Gov't. agencies and their contractors;
Administrative/Operational Use; JUN 1968. Other requests shall be referred to Air Force Rocket Propulsion Lab., Edwards AFB, CA 93523.

AUTHORITY

AFRPL ltr 27 Oct 1971

THIS PAGE IS UNCLASSIFIED

AD 835-398

Report No. AFRPL-TR-68-94

**INVESTIGATION OF THE THERMODYNAMIC PROPERTIES OF
ROCKET COMBUSTION PRODUCTS**

Milton Farber and Margaret A. Frisch

FINAL REPORT

Contract F04611-68-C-0020

June 1968

**Department of the Air Force
Air Force Rocket Propulsion Laboratory (AFSC)
Edwards, California 93523**

**This document is subject to special
export controls and each transmittal to
foreign governments or foreign nationals
may be made only with prior approval of
AFRPL (RPPR-STINFO), Edwards, Calif.
93523.**

**D D C
RECEIVED
JUL 16 1968
REGULATED
C**

When U. S. Government drawings, specifications, or other data are used for any purpose other than a definitely related Government procurement operation, the Government thereby incurs no responsibility nor any obligation whatsoever, and the fact that the Government may have formulated, furnished, or in any way supplied the said drawings, specifications, or other data, is not to be regarded by implication or otherwise, or in any manner licensing the holder or any other person or corporation, or conveying any rights or permission to manufacture, use, or sell any patented invention that may in any way be related thereto.

ACQUISITION NO.	
7/81	WHITE SECTION <input type="checkbox"/>
908	DIFF SECTION <input checked="" type="checkbox"/>
UNANNOUNCED JUSTIFICATION.....	
BY.....	
DISTRIBUCTION/AVAILABILITY CODE	
DIST.	AVAIL. AND/OR SPECIAL
2	

Report No. AFRPL-TR-68-94

**INVESTIGATION OF THE THERMODYNAMIC PROPERTIES OF
ROCKET COMBUSTION PRODUCTS**

Milton Farber and Margaret A. Frisch

FINAL REPORT

Contract F04611-68-C-0020

June 1968

**Department of the Air Force
Air Force Rocket Propulsion Laboratory (AFSC)
Edwards, California 93523**

**Participants:
Milton Farber
Margaret A. Frisch
Hon Chung Ko
George E. Grenier**

**This document is subject to special
export controls and each transmittal to
foreign governments or foreign nationals
may be made only with prior approval of
AFRPL (RPPR-STINFO), Edwards, Calif.
93523.**

FOREWORD

This report presents details of the work performed under Contract No. F04611-68-C-0020 during the period 30 October 1967 through 30 April 1968 at Space Sciences, Inc., 135 W. Maple Ave., Monrovia, California 91016. The principal investigator of this program was Mr. Milton Farber. Dr. Margaret A. Frisch acted as associate investigator and was assisted by Drs. Hon Chung Ko and George Grenier.

The technical monitor of this program was Mr. Curtis C. Selph, RPCL, Air Force Rocket Propulsion Laboratory, Air Force Systems Command, Edwards, California.

This technical report has been reviewed and is approved.

W. H. Ebelke, Colonel, USAF
Chief, Propellant Division

ABSTRACT

A research program has been conducted for the past six months involving molecular flow effusion and mass spectrometric techniques in which thermodynamic properties were obtained for: AlH(g) , $\text{AlH}_2\text{(g)}$, Al(g) , $\alpha\text{AlB}_{12}\text{(c)}$ and $\text{AlB}_2\text{(c)}$.

TABLE OF CONTENTS

	<u>page</u>
I. INTRODUCTION	1
II. THERMODYNAMIC PROPERTIES OF AlH(g) , $\text{AlH}_2\text{(g)}$, and Al(g)	2
A. Introduction	2
B. Experimental	2
1. Apparatus	2
a. Furnace System	2
b. Mass Spectrometer System	4
c. Measurement of Ion Intensity	5
C. Results and Discussion	7
1. Heat of Vaporization of Aluminum	9
2. Heat of Formation of AlH(g)	9
3. Heat of Formation of $\text{AlH}_2\text{(g)}$	10
III. THERMODYNAMIC PROPERTIES OF $\alpha\text{-AlB}_{12}\text{(c)}$ AND $\text{AlB}_2\text{(c)}$	12
A. Introduction	12
B. Experimental	13
1. Apparatus	13
2. Materials	13
a. Aluminum Dodecaboride, $\alpha\text{-AlB}_{12}\text{(c)}$	13
b. Aluminum Diboride, $\text{AlB}_2\text{(c)}$	14
C. Results and Discussion	14
1. Heat of Formation of $\alpha\text{-AlB}_{12}\text{(c)}$	14
2. Heat of Formation of $\text{AlB}_2\text{(c)}$	15
REFERENCES	19
TABLES	
I. Al^+ Intensities over Al(l) and Equilibrium Constants from 1440°K to 1600°K	20
II. Al^+ and AlD^+ Intensities and Equilibrium Constants for reaction Al(l) with $\text{D}_2\text{(g)}$ between 1430°K and 1630°K	21
III. Aluminum Ion Intensities over $\alpha\text{-AlB}_{12}\text{(c)}$ and Equilibrium Constants between 1240°K and 1560°K , Run 1	22
IV. Aluminum Ion Intensities over $\alpha\text{-AlB}_{12}\text{(c)}$ and Equilibrium Constants between 1240°K and 1560°K , Run 2	23

V.	Aluminum Ion Intensities over $\text{AlB}_2(\text{c})$ and Equilibrium Constants between 1060°K and 1220°K , Sample I	24
VI.	Aluminum Ion Intensities over $\text{AlB}_2(\text{c})$ and Equilibrium Constants between 1060°K and 1220°K , Sample II	25

FIGURES

1.	Cross Section View of Furnace and Mass Spectrometer Systems	26
2.	Ionization Efficiency Curve for AlD^+	27
3.	Plot of $\log_{10}(I_{\text{Al}} \cdot T)$ vs $1/T$ representing the reaction $\text{Al}(\text{l}) = \text{Al}(\text{g})$	28
4.	Plot of $\log_{10}(I_{\text{AlD}}/I_{\text{Al}})$ vs $1/T$ representing the reaction $\text{Al}(\text{g}) + 1/2\text{D}_2(\text{g}) = \text{AlD}(\text{g})$, $\text{D}_2 = 10^{-4}$ atm (const.)	29
5.	Plot of $\log_{10}(I_{\text{AlD}} \cdot T)$ vs $1/T$ representing the reaction $\text{Al}(\text{l}) + 1/2\text{D}_2(\text{g}) = \text{AlD}(\text{g})$, $\text{D}_2 = 10^{-4}$ atm (const.)	30
6.	Phase Diagram	31
7.	Plot of $\log_{10}(I_{\text{Al}} \cdot T)$ vs $1/T$ representing the reaction $\alpha\text{AlB}_{12}(\text{c}) = \text{Al}(\text{g}) + 12\text{B}(\text{c})$	32
8.	Plot of $\log_{10}(I_{\text{Al}} \cdot T)$ vs $1/T$ representing the reaction $\text{AlB}_2(\text{c}) = \text{Al}(\text{g}) + 2\text{B}(\text{c})$	33
9.	Al^+ Intensities from a sample of $\text{AlB}_2(\text{c})$ heated from $1060 - 1510^\circ\text{K}$	34

I. INTRODUCTION

The extensive research and development efforts in the area of high energy propellant systems, solid, liquid and hybrid, have led to consideration of an increasingly large number of compounds containing an ever-widening spectrum of the elements. The accurate theoretical evaluation of these new propellant systems in terms of specific impulse, range and similar parameters, requires a knowledge of the thermodynamic properties of the reactants (heat of formation, ΔH_f , is the prime requisite here) and the thermodynamic and physical properties of the possible products. Among the values required are heat of formation, entropy, heat capacity, melting point, and heats of vaporization, fusion and sublimation. Since rocket exhaust temperatures are in the range 2000-5000^oK, generally, the thermodynamic properties of the exhaust products must be known in this temperature range.

The existence of thermodynamic data, whether theoretical or experimental, in the range of 20-600^oK for a given compound is not sufficient to permit the accurate theoretical evaluation of a propellant system which on combustion might form this compound at temperatures of 3000^oK. Extrapolation of thermodynamic data over these temperature spans, i.e. 600 to 3000^oK, are frequently inaccurate. More importantly, large numbers of species produced in propellant combustion do not even exist at lower temperatures and thus their properties can only be determined at the high temperatures where they are formed. It is for these reasons that a research program has been undertaken in this laboratory to determine the physical and thermodynamic properties of those species expected to be formed by the combustion of propellants.

During the past six months experimental studies were conducted for the reactions of (1) Al(l) with D₂(g); (2) the decomposition of AlB₂(c) and AlB₁₂(c). As a result thermal data have been obtained for the following compounds:



All thermodynamic values reported at 298^oK as well as those at the specified temperatures were calculated employing the latest JANAF Tables¹ except where indicated in the text.

II. THERMODYNAMIC PROPERTIES OF $\text{AlH}(\text{g})$, $\text{AlH}_2(\text{g})$ AND $\text{Al}(\text{g})$

A. Introduction.

Experimental evidence for the heat of formation of $\text{AlH}(\text{g})$ is based on the molecular spectra data reported by A. G. Gaydon.² His extrapolation of the vibrational levels gives 2.9 ± 0.2 eV for the best value of D_0° or 62 ± 5 kcal/mole for ΔH_{f298}° . However, a linear Birge-Spencer extrapolation of the same spectra data yields 3.05 eV for D_0° . No experimental or estimated values have been reported for the heat of formation of $\text{AlH}_2(\text{g})$.

Since no experimental measurements are reported for the D_0° of $\text{AlH}(\text{g})$, an effusion-mass spectrometric study was undertaken on the equilibrium reactions involving deuterium gas and aluminum liquid over the temperature range 1430 to 1630°K. Deuterium gas was chosen instead of hydrogen due to background interference at mass 28 where the AlH^+ ion would appear.

B. Experimental

1. Apparatus

The experimental apparatus consisted of two major sections: the high temperature double furnace, mounted in its own vacuum chamber (2×10^{-8} mm Hg), for heating the effusion cells to temperatures up to 2500°K; and the mass spectrometer vacuum chamber in which the quadrupole mass spectrometer (Electronic Associates, Inc. Model Quad 200) is held in a high vacuum (1×10^{-9} mm Hg).

a. Furnace System

(1) Vacuum Chamber

The furnace chamber was fabricated in a cross configuration using 304L stainless steel 12" and 3 1/2" schedule 10 pipe and 3/8" thick plate. All seams were heli-arc welded on the inside to minimize the outgassing load. The mass spectrometer system sealed off one end of the 12" pipe, while the other 12" flange supported the furnace assembly. The cross was attached to the pumping system via one of the 3 1/2" sidearms while the other was sealed by a plate flange containing a 2" quartz window to permit visual temperature measurement. Only viton O-rings and teflon ferrules were used as seals. The cross section drawing of the chamber is presented in Fig. 1.

During furnace operation the 12" pipe was cooled with freon 22 which was expanded through a coil of 5/8" copper tubing soldered to the outside surface of the 12" pipe while each 12" flange was air cooled using high speed blowers.

The furnace chamber was evacuated by a 4" high speed NRC diffusion pump (750 l/sec), charged with Dow Corning 705 oil. The diffusion pump is backed by a Welch Duo-Seal two stage forepump (100 l/min). Both an NRC expanded water cooled chevron baffle and a 4" Veeco cold trap were included in the system.

(2) Furnace

Each heating element of the double furnace consisted of twelve high density graphite rods (1 3/4" long by 1/8" diam., resistivity 1.5×10^{-3} ohm cm^{-1}) connected in series via eleven 1/4" diam. coupling rods. These couplers joined the 1/8" rods at alternate ends to provide a separation of 0.386" between centers. This distance is equivalent to a 30° chord of a 1 1/2" diam. circle. The resistance at room temperature of each element was approximately 1.0 ohm.

The radiation shielding was a set of nine nested cylinders, fabricated from 5 mil tantalum sheet. The shield diameters ranged from 2 1/2" to 4 1/2" with the corresponding lengths changing from 7" to 8 1/2", which gave a uniform 1/8" spacing between shields. The cylinders were supported by three 1/8" rods which passed radially through the shields at 120° intervals around each end. These rods terminated in three 1/2" diam. stainless steel rods that held the shield system 4" off the flange. These shields were kept rigid and concentric by .120" thick graphite annular spacers placed between each shield on these 1/8" rods. The cylinder ends were closed by a mating stack of discs. The top stack was provided with a 1/2" hole which was coaxial with both the mass spectrometer ionizer and reaction cell orifice while the bottom set had a 3/4" hole to permit the reaction cell to pass into the furnace. The shielding was divided into two equal chambers by nine 2 1/2" diam. discs, each having a 3/4" hole on center.

(3) Temperature Measurement and Control

Power for the heating element was supplied by

a 45 amp 0-230V Variac for temperatures above 1800^oK and by a 64 amp 0-30V transformer for temperatures below 1800^oK. The cell temperature was measured by sighting through a set of 1/4" holes in the cylindrical shields, coaxial with the viewing port, with a factory calibrated Pyro Micro Optical Pyrometer. The filament current, corresponding to a given temperature, was read as the voltage drop across a 1 ohm standard resistor on a Leeds & Northrup millivolt potentiometer. The temperature resolution at 1000^oC was approximately 1/2 degree. The shield system was very effective in producing near black body conditions since both the BeO and graphite cells showed nearly identical temperatures at the same power setting. The temperature was stable to within 1 to 2 degrees at a constant power level.

(4) Reaction Cells and Flow System

The reaction cell and gas flow tube were mounted on a separate flange which was sealed to the center of the main furnace flange via a viton O-ring. This arrangement facilitated the maintenance of the reaction system without disturbing the furnace assembly. The BeO reaction cell (orifice dimensions: .92 mm diam., 6.8 mm long) used in the aluminum diboride and aluminum hydride studies was joined to a molybdenum flow tube (.25" o.d. x .19" i.d.) via a molybdenum bushing. In the AlB₁₂ studies a graphite cell (orifice dimensions: 1.01 mm diam., 5.3 mm long) was employed.

The D₂ reaction gas for the AlD experiments was reduced from the high cylinder pressure to 0.1 atm by expansion into a 2 liter ballast tank, which was previously baked out and evacuated via an auxiliary vacuum system (5 x 10⁻⁷ mm Hg). The 2 liter volume of the reservoir tank was large enough so that the gas flow rate at a 100 micron cell pressure resulted in less than a 1% change in tank pressure after one hour. This arrangement minimized the number of adjustments to the Granville-Phillips variable leak valve during a run to maintain a constant D₂ pressure in the cell. The gas pressure in the flow tube was monitored by a calibrated Veeco DV-1 thermocouple gauge.

b. Mass Spectrometer System

(1) Vacuum Chamber

This chamber was constructed in a cross configuration using 5" and 3 1/2" 304L stainless steel pipe. The pumping

system was joined to this chamber via the 5" pipe, giving maximum conductance for evacuation of the chamber. The mass spectrometer probe was mounted to one of the 3 1/2" arms while the second was welded closed with a 12" flange. This flange, which was common to the furnace chamber, had a 1/4" hole on center to permit the molecular beam from the effusion cell to enter the mass spectrometer chamber. This hole could be sealed by rotating a stainless steel bar containing a viton O-ring and drawing the bar flush with the flange surface. This valve provided flexibility in bringing the furnace chamber and reaction system to atmospheric pressure without having to pressurize the mass spectrometer chamber. All seals in the system were metal to provide the highest possible vacuum. The pumping system consisted of a 4" CVC diffusion pump charged with Dow Corning 705 oil, a 4" Granville-Phillips Cryosorb cold trap and a Cenco Hyvac 7 forepump. The vacuum in the chamber without bakeout was between $1 - 2 \times 10^{-9}$ mm Hg.

(2) Quadrupole Mass Spectrometer

The quadrupole mass spectrometer used in this study (Model Quad 200 manufactured by Electronic Associates, Inc.) had a resolution of 500 and a sensitivity of 10^{-14} torr for N_2 , when an electron multiplier was used in conjunction with an electrometer amplifier. The quadrupole probe, factory mounted on a 4" Ultek flange, projected approximately 9" into the vacuum system.

c. Measurement of Ion Intensity

The detection of a gas specie in a molecular beam by mass spectrometric measurement was limited by the interference of background gases at the same m/e number. Since the molecular beam cross section was only a fraction of 4π steradians at the ionizer ($\sim 10^{-4}$) the effective specie "pressure" in the beam was consequently attenuated by this factor relative to the background gases. However, there were several means available to improve the signal level over the background level:

1. By providing separate pumping systems for both the mass spectrometer chamber and the furnace chamber where the molecular beam originates, the residual gases in the mass spectrometer chamber could be held at the lowest possible level. In the present experimental arrangement a 200 fold pressure difference could be maintained between the two chambers.

2. The gas effusing from the reaction cell must reach the ionizer in a collision free trajectory in order to generate a meaningful signal. Those molecules which leave the cell at off axis angles ($> \pm 1.50^\circ$) were not effective in producing a signal but contributed to the background pressure in the furnace and a proportional amount in the mass spectrometer chamber. Since the noise interference at a given peak was dependent directly on the d.c. level generated by these background gases, a reduction of these off axis molecules improved the signal to noise ratio considerably. These off axis molecules were attenuated by the use of 1/4" long orifices in the reaction cells.

3. To distinguish the beam from the background level a simple scheme of manually rotating a sector in the beam path was employed initially. However, this technique required considerable arduous labor to obtain ion intensities for many species at several temperatures. This was replaced by a rotating chopper and a highly sensitive detection system. The molecular beam was mechanically chopped by a two-bladed shutter rotating at a speed of 15 rps. This sector was driven externally by a Bodine 1800 rpm synchronous motor via a rotary seal and a 2:1 gear reduction using Pic Design non-slip pulley and gears. The rotary seal, designed in this laboratory, contained two precision ball bearings and a double O-ring seal. The intervening space between the seals was pumped to 30 microns as a precautionary measure in case of a seal failure while the furnace was at a high temperature.

Ion currents, which originated from species in the molecular beam, appeared as a 30 cps square wave while background gases continued to exist as a d.c. current. The output from the electron multiplier was amplified by a Keithly electrometer amplifier Model 300, incorporating a series of feedback resistors from 10^6 to 10^9 ohms. The band pass of the amplifier was 1 kc at a 3 db attenuation. The output signal from the electrometer amplifier was fed to a Princeton Applied Research Model JB4 lock-in amplifier. Any signal which was in phase with the "open" time of the chopper was integrated at the output. Integration time constants up to 65 sec could be selected to average random ion noise.

The reference signal for the lock-in amplifier

was derived from a signal generated by passing two miniature magnets past a magnetic recording head. These magnets were held radially in an aluminum disc, attached to the shaft of the motor. Minor adjustments in the phase angle were effected by a delay circuit in the reference wave generator.

The detection limit of the electron multiplier current achieved under these conditions was 5×10^{-14} amp, which is equivalent to a few ions per second arriving at the electron multiplier. In addition, a 30 cps current could be detected in a dc signal 1000 times greater.

To ascertain the beam density of the chopped ion a sector with several holes ranging from 1/16" to 7/32" in 1/32" steps could be placed in the beam path. Species which originated solely from the cell showed no significant attenuation with hole sizes 1/8" and above. This sector was approximately 3" from the reaction cell. During the studies reported here the aperture was kept at 1/8".

C. Results and Discussion

Employing a deuterium pressure of 10^{-4} atm over liquid aluminum in the temperature range 1100 to 1630°K the only ions which gave a detectable signal were D^+ , D_2^+ , Al^+ and AlD^+ . No peak attributable to AlD_2^+ could be distinguished over the background noise, even up to a D_2 pressure of 5×10^{-4} atm. In the temperature range studied the D^+ ion is a fragment from D_2 . Also, no other species involving Al and D were observed.

The AlD^+ ion ($m/e = 29$) was observed over the temperature range 1430 to 1630°K at an intensity level of approximately 1% of the aluminum ion intensity ($m/e = 27$). The appearance potential for AlD^+ was determined from the ionization efficiency curve (see Fig. 2) to be 7.9 eV, which is in agreement with the estimate of 7.95 eV made by Grimaldi³ based on molecular spectroscopy data. Measurements of the ion intensity at mass 27 and mass 29 were made at 0.6 ma emission current and 12 volts electron energy. The electron energy of twelve volts was established as the optimum value for the best signal to noise ratio at masses 27 and 29. However, the appearance potential for D_2^+ is 15.4 eV, which would necessitate making ion current

measurements at two widely varying electron energy settings, i.e., 12 and 20 volts. Previous experience with the mass spectrometer ionizer has demonstrated that a long duration is required to establish a stable ion current reading when the electron energy is altered. Thus the D_2 gas pressure was held constant throughout the experiments by adjustment of the variable leak valve.

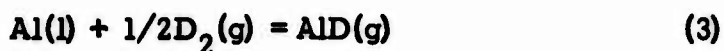
The following equilibrium reactions were considered for the interpretation of the ion intensity data.



$$K_1 = I_{Al}^+ \cdot T$$



$$K_2 = I_{AlD}^+ / I_{Al}^+$$



$$K_3 = I_{AlD}^+ \cdot T$$

The deuterium ion intensity was not included in equilibrium constants (2) and (3) since its pressure was held constant during the experiments.

To verify that D_2 was in equilibrium with $Al(l)$ according to reaction (3), the D_2 pressure was varied over a factor of 15 from 10^{-4} atm to 7×10^{-6} atm. The ion intensity of AlD^+ was correspondingly reduced by a factor of 3.7, which is in reasonable agreement with the expected factor of 3.9 from reaction (3).

Since the heat of formation of AlD is highly dependent on the heat of vaporization of Al (reaction (1)), this equilibrium was studied without the presence of D_2 gas. The ion intensity data and equilibrium constants from this study are presented in Table I. A plot of $\log_{10} K_1$ vs $1/T$ is shown as run 3 in Fig. 3.

Two studies were made with D_2 gas present, the first with rising temperature and the second with decreasing temperature. These ion current data and equilibrium constants for reactions (1), (2) and (3) are presented in Table II. Figures 3, 4 and 5 show the second law plots for reactions (1), (2) and (3).

In addition to these mass spectrometric measurements, the absolute vapor pressure of aluminum was determined from a Knudsen effusion experiment. At 1578°K , 4.05 mg of aluminum effused from the BeO cell during 280 minutes. From the cell geometry (effective orifice area = $9.2 \times 10^{-4} \text{ cm}^2$ calculated from cell geometry and Clausing factor) this weight loss corresponds to an aluminum vapor pressure of $4.5 \times 10^{-5} \text{ atm}$, while the JANAF tabulation on Al(g) gives $5.6 \times 10^{-5} \text{ atm}$ at 1578°K .

1. Heat of Vaporization of Aluminum

The three second law results for reaction (1) are in good agreement with each other, their values being 71.9 ± 0.5 (no D_2 present), 75.0 ± 0.9 and $73.5 \pm 1.8 \text{ kcal/mole}$ at the average temperature of 1525°K . The uncertainty of the slope is the statistical error and does not represent the actual confidence limit. Reduction of the average of these three values ($73.5 \pm 1.5 \text{ kcal/mole}$) to 298°K yields $78.8 \pm 1.5 \text{ kcal/mole}$ for the heat of formation of Al(g). This is in good agreement with the value of $78.0 \pm 0.9 \text{ kcal/mole}$ reported in the JANAF Tables.¹ Recently, Potter⁴ by means of the torsion effusion method obtained a second law value of $80.3 \pm 1.2 \text{ kcal/mole}$ for $\Delta H_{f298^\circ\text{K}}^\circ$ of Al(g).

2. Heat of Formation of AlH(g)

The two series of effusion-mass spectrometric experiments yielded -19.6 ± 1.0 and $-20.1 \pm 0.5 \text{ kcal/mole}$ for the heat of reaction (2) at 1525°K while for reaction (3) values of 54.8 ± 0.4 and $53.3 \pm 1.5 \text{ kcal/mole}$ were obtained. (The uncertainties of the slopes are the statistical error only.) Since reaction (3) gives directly the heat of formation of AlD(g), it was employed exclusively for this thermodynamic quantity. The average of the two runs of $54.0 \pm 1.5 \text{ kcal/mole}$ at 1525°K reduces to $59.5 \pm 2.5 \text{ kcal/mole}$ at 298°K . This value is in agreement with the spectroscopic value of 62.0 kcal/mole .

Within the experimental error this value is valid for AlH(g) since the deuterium bond stability is within one kcal of that of the hydrogen bond for most known deuterium compounds (i.e., D₂O is more stable than H₂O by 1.8 kcal).

A third law analysis of the data was made employing the 1593.5°K point in run 3. The cross sections for Al and AlD are assumed to be essentially identical. The change in mass spectrometer sensitivity with mass over this interval is negligible.

$$K'_2 = \frac{I_{\text{AlD}}^+}{I_{\text{Al}}^+ \cdot (D_2)^{1/2}} \quad (4)$$

Since Al⁺ ion was measured 6 volts above its appearance potential while AlD⁺ was 4 volts above, a 1.5 factor was applied to the values of K₂ taken from Table II to correct it to the same electron energy difference.

Thus, at the temperature of 1593.5°K and for a pressure of D₂ of 10⁻⁴ atm

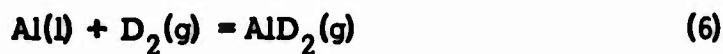
$$K'_2 = \frac{(4.60 \times 10^{-3}) (1.5)}{10^{-2}} = 0.69 \text{ atm}^{-1/2} \quad (5)$$

This yields a third law ΔH_{f298}° for AlH(g) of 63.0 kcal/mole.

3. Heat of Formation of AlH₂(g)

In an attempt to obtain a mass spectrometric identification of the AlH₂ molecule, experiments involving D₂ gas and Al liquid were performed at pressures up to 5 x 10⁻⁴ atm and at a temperature of 1550°K. Under these optimum conditions no positive identification of a peak at m/e = 31 could be made. The modulated ion current was measured repeatedly at masses 31 and 31.5 for a period of approximately 10 minutes each, using a time constant of 60 seconds to give maximum signal to noise ratio. There

was no discernible ion current difference between these two mass settings up to a detection limit of 1 part in 70,000 of the aluminum ion current. At 1550°K the Al(g) pressure is about 3.5×10^{-5} atm. Assuming the AlD₂ parent ion would exist, the lower detection limit for AlD₂(g) in the present study is approximately 5×10^{-10} atm. Based on the following equation



an equilibrium constant of 10^{-6} is obtained. This is equivalent to a free energy of formation for AlD₂(g) more positive than +42.5 kcal/mole. The entropy of AlD₂(g) at 1550°K has been estimated as 65.0 e.u. based on an analogy with BH₂. The resultant heat of formation of AlD₂(g) is more positive than 44.3 kcal/mole at 1550°K and 50 kcal/mole at 298°K.

The transpiration study for the reaction of Al(l) with H₂(g) at 1 atm was not attempted since three materials would be competing for the weight loss resulting from aluminum, i.e., Al(g), AlH(g), and possibly AlH₂(g). Employing the mass spectrometric data as a criterion the weight loss resulting from the formation of AlH₂(g) would be approximately 10% of the total.

III. THERMODYNAMIC PROPERTIES OF $\alpha\text{AlB}_{12}(\text{c})$ AND $\text{AlB}_2(\text{c})$

A. Introduction

The solid phases of aluminum and boron are complicated and result in several stable compounds of varying compositions. Aluminum diboride, AlB_2 , has been prepared by Felten⁵ in almost pure form by heating stoichiometric amounts of aluminum and boron to 1073°K . However, the x-ray diffraction analysis showed some free aluminum present. Duhart⁶ studied the synthesis of AlB_2 and found that its formation was critical with temperature. At a synthesis temperature of 1023°K the x-ray analysis showed weak AlB_2 lines and very strong aluminum lines. He also verified Felten's work that 1073°K to 1093°K is the most probable temperature range for the synthesis of AlB_2 . X-ray diffraction data at both these temperatures showed strong AlB_2 lines with considerable aluminum line structure. At a synthesis temperature of 1123°K to 1223°K the AlB_2 x-ray structure becomes weaker and weaker with the aluminum increasing in strength and at 1223°K no AlB_2 is found. He concluded that above 1223°K AlB_2 is disproportionating to αAlB_{12} . This has also been recently verified by Serebryanskii, et al,⁷ who showed that above 1248°K AlB_2 disproportionates into αAlB_{12} . From these published reports Elliot⁸ constructed a phase diagram (see Fig. 6) showing the stable phases of the aluminum boron system. The stable phase of αAlB_{12} is shown as between 1248 to 1723°K . Above this temperature αAlB_{12} decomposes to βAlB_{12} .

Very little thermodynamic data has been reported for the aluminum borides. Armstrong and Domalski⁹ measured the heats of combustion in fluorine of AlB_2 , αAlB_{12} , and γAlB_{12} . Though the measurements were of high precision, the chemical analysis was not entirely satisfactory. This class of compounds has a broad range of non-stoichiometric compound formation.¹⁰ Thus an analysis which might be adequate to assign a formula to a stoichiometric compound is inadequate for assignment of a composition to a non-stoichiometric compound. The choice of composition in some cases caused a three kcal/mole difference in the heat of formation. The authors indicated that a difference of 22 kcal/mole could be partly or wholly due to error of analysis. Using the interpretation of non-stoichiometry and a distribution of non-metallic impurities in accordance with the Al/B mole

ratio, Armstrong and Domalski⁹ reported the following heats of formation at 298°K in kcal/mole: -16.2 for $\text{AlB}_{2.213}$, -61.3 for $\alpha\text{AlB}_{11.96}$, and -37.9 for $\gamma\text{AlB}_{12.57}$. Samsonov, et al,¹¹ measured the Langmuir vapor pressure of AlB_{12} and found that it decomposed into the elements. They reported the heat of reaction as 45.7 kcal/mole, which yields a heat of formation for AlB_{12} of approximately 25 kcal/mole at 298°K. In view of their positive heats of formation for ZrB_2 and TiB_2 , which JANAF reports to be of negative sign and some 150 kcal/mole lower, their value for AlB_{12} may be disregarded.

To obtain clarification of the thermodynamic properties of the aluminum borides, a molecular flow effusion-mass spectrometric study was conducted in this laboratory. The compounds chosen for study were $\text{AlB}_2(\text{c})$ and $\alpha\text{AlB}_{12}(\text{c})$, which were obtained commercially. A preliminary mass spectrometric investigation of the decomposition temperatures of these compounds essentially verified the phase structure shown in the phase diagram (Fig. 6). Thus, studies were made for the heat of formation of AlB_2 in the temperature range of 1060 to 1220°K and for αAlB_{12} in the temperature range 1200 to 1560°K.

Since very little thermodynamic data are reported on the several aluminum borides the experimental measurement of the entropy of AlB_2 and αAlB_{12} was desirable. This necessitated the obtaining of both absolute ion intensity measurements and effusion weight loss data.

B. Experimental

1. Apparatus

The description of the experimental apparatus is given in Section II.B. of this report.

2. Materials

a. Aluminum Dodecaboride, $\alpha\text{AlB}_{12}(\text{c})$

A sample of $\alpha\text{AlB}_{12}(\text{c})$ (min. purity 96%) was obtained from Alfa Inorganics, Inc. with the following analysis in weight percent:

Al	18.20%	C	0.80%
B	78.81%	Mg	0.05%
Fe	0.05%	Zr	0.10%
Si	0.20%	Unaccounted:	1.8%

Stoichiometry of the sample indicates $\text{AlB}_{10.81}$, or 95.2% AlB_{12} . X-ray analysis was performed on the sample by Edwards Air Force Base before and after heating and showed only αAlB_{12} to be present. Samples were ground to a uniform particle size and loaded into a 0.3 mm i.d. glass capillary and mounted in a 57.3 mm Debye-Scherrer powder x-ray diffraction camera. A one-hour exposure was taken of each sample using nickel-filtered copper radiation. The effusion-mass spectrometric studies were made in a high density graphite cell.

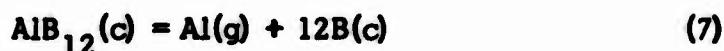
b. Aluminum diboride, $\text{AlB}_2(\text{c})$

This material was also obtained from Alfa Inorganics, Inc. and had a typical analysis of Al 53.9%, B 45.3% and unaccounted 0.8%. This composition gives a stoichiometry of $\text{AlB}_{2.10}$, or 97.1% AlB_2 . The analysis of these samples at Edwards Air Force Base showed Al 50.5% and B 44.9%, or AlB_2 as 95%. The residue was not analyzed. X-ray diffraction analysis at Edwards Air Force Base showed strong Al line structures. Since the Al vapor pressures over the heated AlB_2 samples were much lower than that of pure Al, it is assumed that the Al x-ray lines are not due to free Al but may be due to some encapsulated Al in the solid phase. Since the vapor pressure of $\text{Al}(\text{g})$ over AlB_2 is slightly higher than for Al_4C_3 , the graphite cell that was used in the AlB_{12} study was abandoned in favor of the BeO cell for the final measurements presented in this report.

C. Results and Discussion

1. Heat of Formation of $\alpha\text{AlB}_{12}(\text{c})$

An experimental study has been completed for the decomposition of αAlB_{12} in a carbon cell over a temperature range of 1200 to 1560°K, which is shown as Zone II in the phase diagram (Fig. 6). In this region αAlB_{12} decomposes according to the reaction



The ion intensities of aluminum ($m/e = 27$), the equilibrium constants, and the temperatures are presented in Tables III and IV. The plot of $\log(I_{\text{Al}}^+ T)$ versus $1/T$ is shown in Fig. 7, with the least squares line given by the following equation:

$$\log_{10} (I_{Al}^+ \cdot T) = - \frac{118,000 \pm 730}{4.57T} + 24.78 \pm 0.11 \quad (T_{av} = 1400^{\circ}K) \quad (8)$$

The heat of reaction at 1400^oK is 118.0 ± 1.0 kcal/mole.

The calibration of aluminum weight loss versus aluminum ion intensities was made for both the graphite and BeO cells. These resulted in the following pressure-intensity relationships:

For graphite cell:

$$\log_{10} P_{Al}(\text{atm}) = \log_{10} (I_{Al}^+ \cdot T) - 13.15 \pm 0.3 \quad (9)$$

For BeO cell:

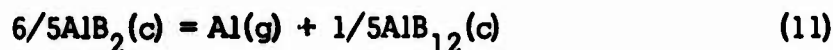
$$\log_{10} P_{Al}(\text{atm}) = \log_{10} (I_{Al}^+ \cdot T) - 13.28 \pm 0.3 \quad (10)$$

Employing equation (9) for the conversion of ion intensities to absolute pressures, the second law entropy of reaction at 1400^oK is 53.2 ± 1.5 cal/deg/mole. Using the JANAF data the resultant entropy for αAlB_{12} is 103.3 cal/deg/mole at 1400^oK. Using the JANAF value for the heat of vaporization of aluminum we find the heat of formation of $\alpha\text{AlB}_{12}(\text{c})$ to be -44.9 ± 1.0 kcal/mole at 1400^oK. Since no experimental heat content data are available for AlB_{12} from 298^oK to 1400^oK, the heat content was assumed to be equal to the sum of the heat content of the elements.¹² Thus the $\Delta H_{f298^{\circ}K}^{\circ}$ of αAlB_{12} is calculated at -43.0 kcal/mole. The identity of the constituents in reaction (7) has been confirmed by x-ray diffraction analysis. A sample was heated for a short time and identified by x-ray to be αAlB_{12} . Another sample was heated for 10 hours with a weight loss of aluminum that represented 50% reaction. This sample showed both αAlB_{12} and boron lines. The identification of AlB_{12} lines and boron lines in this sample required careful examination since the similarity of the structures and electron density distribution of these compounds is well documented.¹³ One of the intense lines for tetragonal boron (d = 2.426) increased considerably. Also, several of the other strong tetragonal boron lines were enhanced in the heated sample.

2. Heat of Formation of $\text{AlB}_2(\text{c})$

A study has been made of the thermal decomposition of

AlB₂(c) in a BeO cell. Two separate sets of experiments were performed over the temperature range 1060 to 1220°K (Region I of the phase diagram, Fig. 6). Duhart,⁶ in previous experiments for the synthesis of AlB₂ from stoichiometric amounts of B and Al which were performed at 1173 and 1223°K, reported the formation of some AlB₁₂ along with the synthesis of AlB₂. He dissolved the AlB₂ in HCl and analyzed the residue by means of x-ray diffraction. These x-ray data show lines for both α and β AlB₁₂. Serebryanskii, et al,⁷ state that the decomposition of AlB₂ to AlB₁₂ and Al is complete at temperatures above 1248°K. However, at temperatures below this he also detected the formation of some α AlB₁₂. Thus the evidence in the literature favors the decomposition of AlB₂ as



The first experimental study was made on a sample taken directly from the supplier's container, while the second was performed on a sample that had been heated at 1100°K for 20 hours in a separate vacuum system. This sample had a weight loss of 0.5 mg from an original weight of 20 mg. This corresponds to a 5% loss of aluminum. Since at 1100°K the pressure over liquid aluminum (2.2×10^{-9} atm) is approximately 5 times greater than that over AlB₂(c) (4.0×10^{-10} atm), it is reasonable to conclude that the free aluminum in AlB₂(c) in excess of that predicted from the phase diagram was removed by this procedure. Any excess aluminum impurity still remaining should not cause a change in the heat of reaction, since the 5% loss of aluminum had no effect on the value within the experimental precision of the measurements. The low temperature range chosen for the measurements was necessitated by the instability of the AlB₂(c) phase above 1250°K. (See phase diagram, Fig. 6.) The aluminum pressure over AlB₂(c) in this region is extremely small, varying between 1×10^{-10} atm at 1060°K to 3×10^{-8} atm at 1220°K. Consequently, the measurement of the modulated aluminum ion current on the lock-in amplifier required long integration times to read the lowest pressure of 10^{-10} atm with at least 5% precision.

The ion intensities of aluminum, the equilibrium constants, and the temperatures are presented in Tables V and VI. The plot of $\log(I_{\text{Al}}^+ T)$

vs $1/T$ is shown in Fig. 8. The following two equations represent the least square lines for experiments one and two, respectively.

Experiment 1:

$$\log_{10} (I_{Al}^+ \cdot T) = -\frac{88,600 \pm 720}{4.57T} + 21.49 \pm 0.14 \quad (T_{av} = 1145^\circ K) \quad (12)$$

Experiment 2:

$$\log_{10} (I_{Al}^+ \cdot T) = -\frac{90,100 \pm 340}{4.57T} + 21.65 \pm .07 \quad (T_{av} = 1155^\circ K) \quad (13)$$

The uncertainties given in these equations represent the statistical error and not the confidence limit. The slopes for the two experiments, 88.6 ± 1.0 and 90.1 ± 1.0 kcal/mole, are nearly the same within the experimental precision in the measurement of the ion intensities. The slight shift in the lines was caused by a change in the electron multiplier sensitivity.

Employing equation (10) for conversion of ion intensities to absolute pressures, an average second law entropy of reaction of 38.0 ± 1.5 cal/deg/mole at $1150^\circ K$ is obtained. Employing JANAF data, the standard entropy of $AlB_2(c)$ is 23.6 cal/deg/mole at $1150^\circ K$. This value appears reasonable in comparison with other diborides. Employing an average value of 89.4 ± 1.0 kcal/mole for the heat of reaction, calculations can be made for the heat of formation of AlB_2 from both equations (11) and (12). Employing equation (11) the heat of formation of $AlB_2(c)$ at $1150^\circ K$ is -20.4 ± 1.0 kcal/mole. (The decomposition according to equation (11) appears to be the reaction favored by several of the previous investigators (Felten,⁵ Duhart,⁶ and Serebryanskii⁷)). Employing the same analogy for the heat content as with AlB_{12} , the heat of formation of $AlB_2(c)$ reduces to -18.0 ± 2.3 kcal/mole based on the reaction given by equation (11), in fairly good agreement with Armstrong and Domalski's⁹ value of -16.2 kcal/mole.

Elliot⁸ reports the peritectic point of AlB_2 to be $1248^\circ K$. AlB_2 decomposes at this temperature into a liquid of nearly pure aluminum (see Fig. 6) and solid $\alpha-AlB_{12}$, as given by reaction (11).

This change of phase was verified in experiments in which

AlB₂(c) samples were heated to temperatures above 1300°K. After these samples were heated they were cooled to temperatures of approximately 1100°K; however, the vapor pressure of Al was then different and considerably higher at the same temperature where the vapor pressure had been previously determined, indicating that the sample had possibly undergone a phase change. X-ray analyses made on these samples confirmed the presence of α -AlB₁₂ in agreement with the phase diagram (Zone III, Fig. 6). Figure 9 presents the ion intensities as a function of the reciprocal temperature for a sample of AlB₂(c) heated from 1060 to 1510°K. A change in slope appeared to take place at 1270 ± 10°K. This value is in good agreement with the value of 1248°K reported from phase studies.⁸ Assuming that this represents the peritectic point a calculation was made for the heat of reaction at this temperature. Since at the peritectic point the free energies for the vaporization of Al and decomposition of AlB₂ are equal, then

$$\Delta H_v - T \Delta S_v = \Delta H_r - T \Delta S_r$$

for the vaporization of aluminum and the decomposition of AlB₂(c). Employing the second law entropy of reaction and the JANAF values for the vaporization of Al, ΔH_r is calculated as 87.3 kcal/mole at 1265°K. This value compares favorably with the average measured value of 89.4 ± 1.0 kcal/mole at 1150°K.

REFERENCES

1. JANAF Thermochemical Tables
2. A. G. Gaydon, "Dissociation Energies," 2nd Ed., Chapman Hall, Ltd., London (1953).
3. F. Grimaldi and A. LeCourt, *J. Mol. Spectroscopy* **20**, 341 (1966).
4. N. D. Potter, private communication.
5. E. J. Felten, *J. Am. Chem. Soc.*, **78**, 5977 (1956).
6. P. Duhart, *Ann. Chim. (Paris)* **7**, 361 (1962).
7. V. T. Serebryanskii, V. A. Epel'baum, and G. S. Zhdanov, *Proc. Acad. Sci. USSR, Chim. Sec.* **141**, 1244 (1961).
8. R. P. Elliot, "Constitution of Binary Alloys, First Supplement," McGraw-Hill, Inc., New York, 1965, pg 26.
9. G. T. Armstrong and E. S. Domalski, NBS Report 9389, 136 (1966).
10. H. Bernstein and L. Kaufman, Tech. Report No. AFML-TR-66-193, June 1966, "Development and Application of Methods for Predicting the Temperature-Composition Stability of Refractory Compounds."
11. A. S. Bolgar, T. S. Verkhoglyadova, and G. V. Samsonov, *Izvest. Akad. Nauk. SSSR Otdel Tekh. Nauk. Mit. i Toplivo*, 1961, p 142.
12. H. C. Weber, "Thermodynamics for Chemical Engineers," J. Wiley & Sons, New York, p 5 (1939).
13. J. L. Hoard and R. E. Hughes, "The Chemistry of Boron and its Compounds," Earl L. Muetterties, Ed., Chapter 2, John Wiley & Sons, New York (1967).

TABLE I

Al⁺ INTENSITIES OVER Al(l) AND EQUILIBRIUM CONSTANTS
FROM 1440°K TO 1600°K

T °K	$10^3/T$ deg. K ⁻¹	I_{Al} x 10 ⁻¹³ amp	$K_1 =$ $I_{Al} \cdot T$	$\log_{10} K_1$
1442	.6935	35000	5.05×10^7	7.703
1509.5	.6625	101000	1.52×10^8	8.183
1560	.6410	213000	3.32×10^8	8.522
1594.5	.6272	350000	5.58×10^8	8.746

TABLE II

AI⁺ AND AID⁺ INTENSITIES AND EQUILIBRIUM CONSTANTS FOR REACTION AI(I) WITH D₂(g)
 BETWEEN 1430°K AND 1630°K

T °K	$10^3/T$ deg. K ⁻¹	I _{AI} x 10 ⁻¹³ amp	I _{AID} x 10 ⁻¹³ amp	K ₁ = I _{AI} · T	log ₁₀ K ₁	K ₂ = I _{AID} /I _{AI}	log ₁₀ K ₂	K ₃ = I _{AID} · T	log ₁₀ K ₃
<u>Run 1</u>									
1432	.6983	39500	420	5.66 x 10 ⁷	7.753	1.06 x 10 ⁻²	-1.973	6.01 x 10 ⁵	5.779
1462.5	.6838	65500	595	9.58 x 10 ⁷	7.981	8.55 x 10 ⁻³	-2.068	8.70 x 10 ⁵	5.940
1507	.6636	141000	1025	2.12 x 10 ⁸	8.327	7.26 x 10 ⁻³	-2.139	1.55 x 10 ⁶	6.189
1536	.6510	220000	1300*	3.38 x 10 ⁸	8.528	5.91 x 10 ⁻³	-2.229*	2.00 x 10 ⁶	6.300*
1558	.6418	320000	1850	4.98 x 10 ⁸	8.697	5.78 x 10 ⁻³	-2.238	2.88 x 10 ⁶	6.460
1590.5	.6287	505000	2550	8.03 x 10 ⁸	8.905	5.05 x 10 ⁻³	-2.297	4.06 x 10 ⁶	6.608
1627.5	.6144	790000	3650	1.29 x 10 ⁹	9.109	4.62 x 10 ⁻³	-2.336	5.94 x 10 ⁶	6.674
<u>Run 2</u>									
1630.5	.6133	685000	2760	1.12 x 10 ⁹	9.048	4.03 x 10 ⁻³	-2.395	4.50 x 10 ⁶	6.653
1593.5	.6276	435000	2000	6.93 x 10 ⁸	8.841	4.60 x 10 ⁻³	-2.337	3.19 x 10 ⁶	6.504
1556.5	.6425	270000	1430	4.20 x 10 ⁸	8.623	5.30 x 10 ⁻³	-2.276	2.22 x 10 ⁶	6.347
1531.5	.6529	185000	1100	2.84 x 10 ⁸	8.452	5.95 x 10 ⁻³	-2.226	1.69 x 10 ⁶	6.227
1510.5	.6620	127000	820	1.92 x 10 ⁸	8.282	6.46 x 10 ⁻³	-2.190	1.24 x 10 ⁶	6.093
1474	.6784	68500	535	1.01 x 10 ⁸	8.004	7.81 x 10 ⁻³	-2.107	7.88 x 10 ⁵	5.897
1438	.6954	35500*	345	5.11 x 10 ⁷	7.708*	9.71 x 10 ⁻³	-2.013*	4.96 x 10 ⁵	5.696

*Discarded

TABLE III

ALUMINUM ION INTENSITIES OVER $\propto \text{AlB}_{12}(\text{c})$ AND EQUILIBRIUM CONSTANTS
BETWEEN 1240°K AND 1560°K

Run 1

T °K	$10^3/T$ deg. K ⁻¹	I_{Al} x 10 ⁻¹³ amp	$K_1 =$ $I_{\text{Al}} \cdot T$	$\log_{10} K_1$
1237.5	.8081	9	1.11×10^4	4.047
1281	.7806	39	5.00×10^4	4.699
1330.5	.7516	162	2.16×10^5	5.333
1368	.7310	510	6.98×10^5	5.844
1405.5	.7115	1640	2.31×10^6	6.363
1461.5	.6842	8100	1.18×10^7	7.073
1514	.6605	38000	5.75×10^7	7.760
1562	.6402	122000	1.91×10^8	8.280
1540	.6494	72000	1.11×10^8	8.045
1514	.6605	39500	5.98×10^7	7.777
1490	.6711	21700	3.23×10^7	7.509
1462.5	.6838	10800	1.58×10^7	7.198
1450.5	.6894	7400	1.07×10^7	7.031
1413	.7077	2550	3.60×10^6	6.556
1390	.7194	1200	1.67×10^6	6.222
1349	.7413	345	4.65×10^5	5.668
1331	.7513	170	2.26×10^5	5.354
1281	.7806	39	5.00×10^4	4.699

TABLE IV

ALUMINUM ION INTENSITIES OVER α - AlB_{12} (c) AND EQUILIBRIUM CONSTANTS
 BETWEEN 1240°K AND 1560°K

Run 2

T °K	$10^3/T$ deg. K ⁻¹	I_{Al} x 10 ⁻¹³ amp	$K_1 =$ $I_{\text{Al}} \cdot T$	$\log_{10} K_1$
1255.5	.7965	10	1.26×10^4	4.099
1288	.7764	43	5.54×10^4	4.743
1319.5	.7579	128	1.69×10^5	5.227
1352.5	.7394	355	4.80×10^5	5.681
1384	.7225	1080	1.49×10^6	6.174
1414.5	.7070	2650	3.75×10^6	6.574
1456.5	.6866	8100	1.18×10^7	7.072
1484	.6739	19800	2.94×10^7	7.468
1517	.6592	46000	6.98×10^7	7.844
1560.5	.6408	126000	1.97×10^8	8.294
1551	.6447	87000	1.35×10^8	8.130
1495	.6689	22500	3.36×10^7	7.527
1474	.6784	12600	1.86×10^7	7.269
1447	.6911	5800	8.39×10^6	6.924
1402.5	.7130	1680	2.36×10^6	6.372
1371	.7294	660	9.05×10^5	5.956
1326	.7541	166	2.20×10^5	5.342
1295	.7722	63	8.16×10^4	4.912
1263	.7918	22	2.78×10^4	4.444
1259	.7943	17	2.14×10^4	4.330
1555.5	.6429	95000	1.48×10^8	8.169

TABLE V

ALUMINUM ION INTENSITIES OVER AlB_2 (c) AND EQUILIBRIUM CONSTANTS
BETWEEN 1060°K AND 1220°K Sample I*

Run No.	T °K	$10^3/T$ deg. K^{-1}	I_{Al} $\times 10^{-13}$ amp	$K_1 =$ $I_{\text{Al}} \cdot T$	$\log_{10} K_1$
1	1146	.8726	32.5	3.72×10^4	4.570
	1168.5	.8558	67	7.82×10^4	4.893
	1189.5	.8407	134	1.59×10^5	5.202
	1215	.8230	285	3.46×10^5	5.540
2	1106	.9042	8.0	8.85×10^3	3.947
	1125	.8889	17	1.91×10^4	4.281
	1145	.8734	36	4.12×10^4	4.615
	1168.5	.8558	69	8.06×10^4	4.906
	1196	.8361	172	2.06×10^5	5.313
	1218.5	.8207	345	4.21×10^5	5.624
	1102	.9074	7.9	8.71×10^3	3.940
	1080	.9259	3.3	3.56×10^3	3.552
	1061	.9425	1.7	1.81×10^3	3.256
	1126	.8881	17.2	1.94×10^4	4.288
	1150.5	.8692	41.0	4.72×10^4	4.674

*Original sample

TABLE VI

ALUMINUM ION INTENSITIES OVER AlB_2 (c) AND EQUILIBRIUM CONSTANTS
 BETWEEN 1060°K AND 1220°K

Sample II*

Run No.	T $^\circ\text{K}$	$10^3/T$ deg. K^{-1}	I_{Al} $\times 10^{-13}$ amp	$K_1 =$ $I_{\text{Al}} \cdot T$	$\log_{10} K_1$
1	1153	.8673	33.5	3.86×10^4	4.586
	1161.5	.8610	41.5	4.82×10^4	4.683
	1192.5	.8386	116	1.38×10^5	5.144
	1210.5	.8261	200	2.42×10^5	5.384
	1212.5	.8247	212.5	2.58×10^5	5.411
	1096	.9124	4.6	5.05×10^3	3.703
2	1166	.8576	50	5.83×10^4	4.766
	1184.5	.8442	89	1.05×10^5	5.023
	1208.5	.8274	188	2.27×10^5	5.356
	1186	.8432	92.5	1.10×10^5	5.040
	1151.5	.8684	31	3.57×10^4	4.553
	1135	.8811	18	2.04×10^4	4.310
	1121	.8921	10.6	1.19×10^4	4.075
	1098	.9107	4.7	5.16×10^3	3.712
	1078	.9276	2.2	2.37×10^3	3.374

*Original sample preheated 20 hrs at 1100°K in open cell

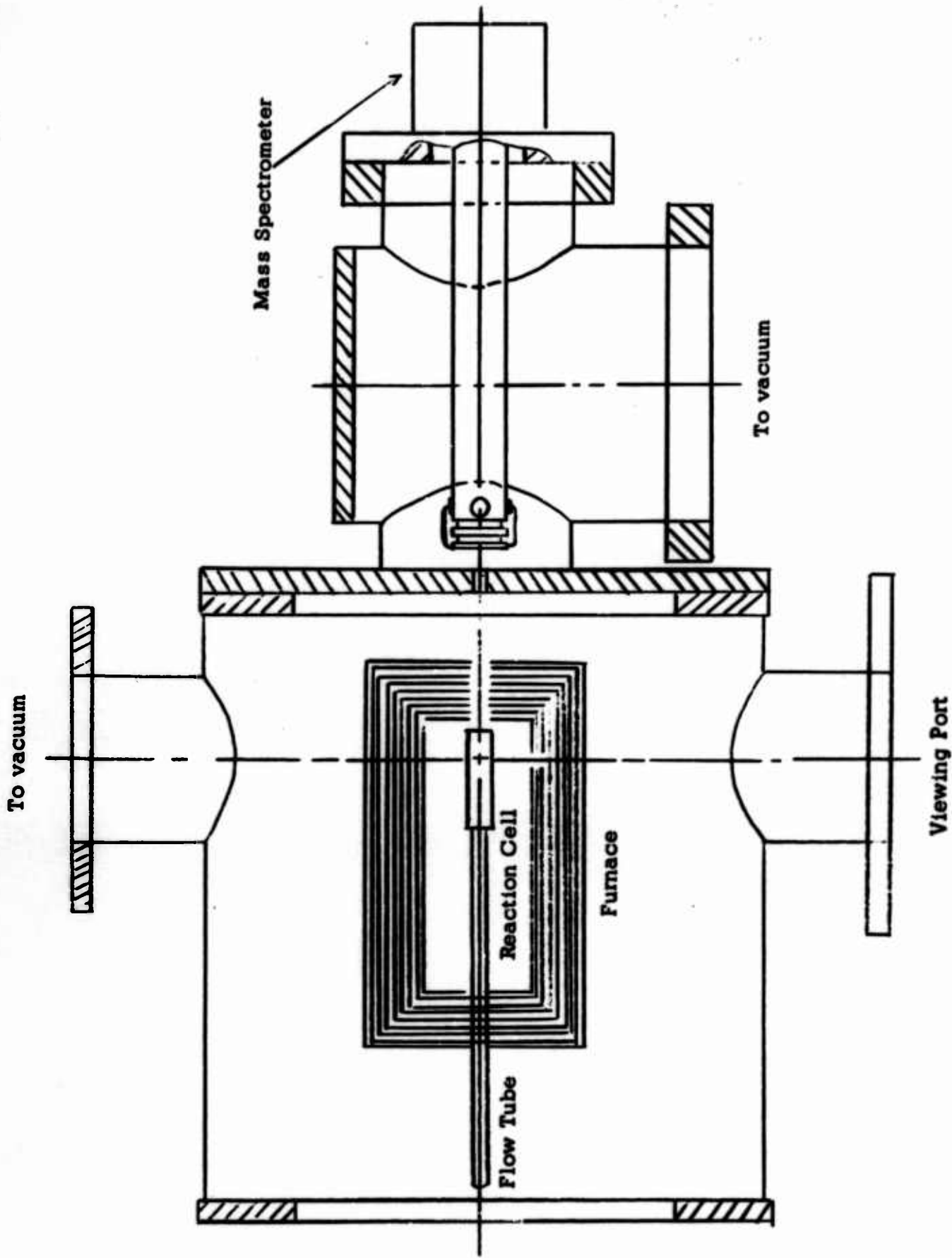


Fig. 1. Cross Section View of Furnace and Mass Spectrometer Systems

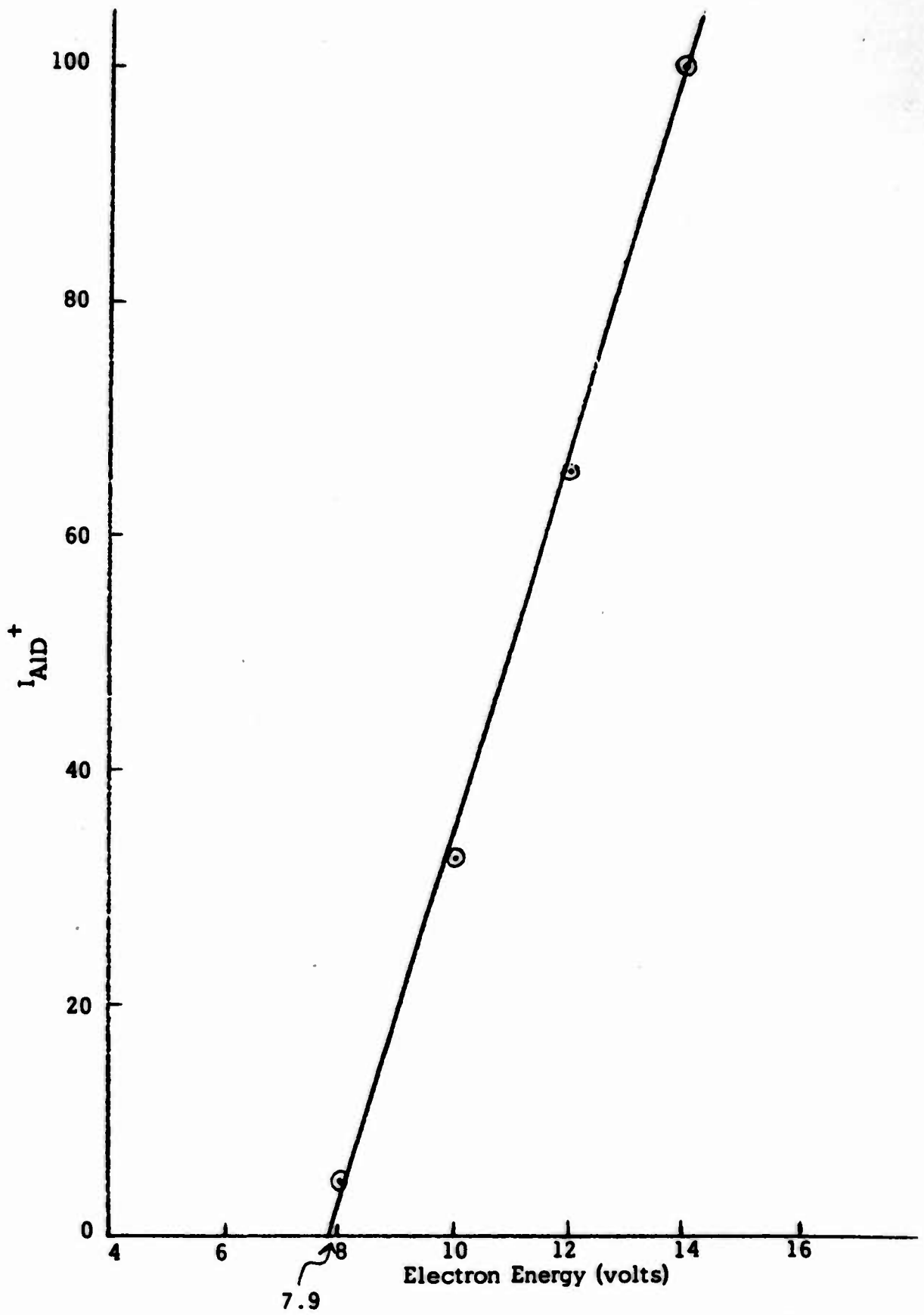


Fig. 2. Ionization Efficiency Curve for AID^+

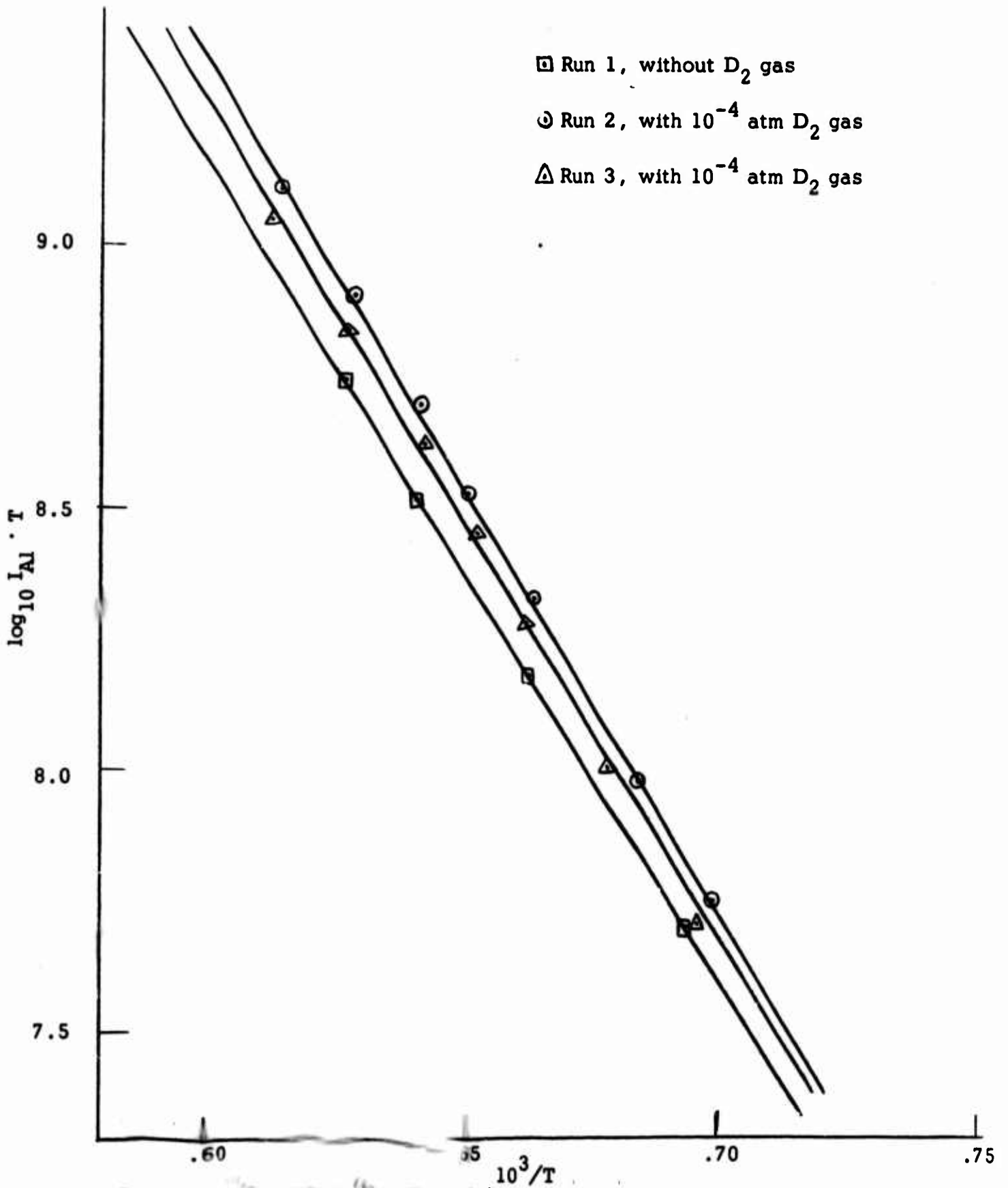


Fig. 3. $\log_{10} I_{Al} \cdot T$ vs $1/T$ representing the reaction $Al(l) = Al(g)$

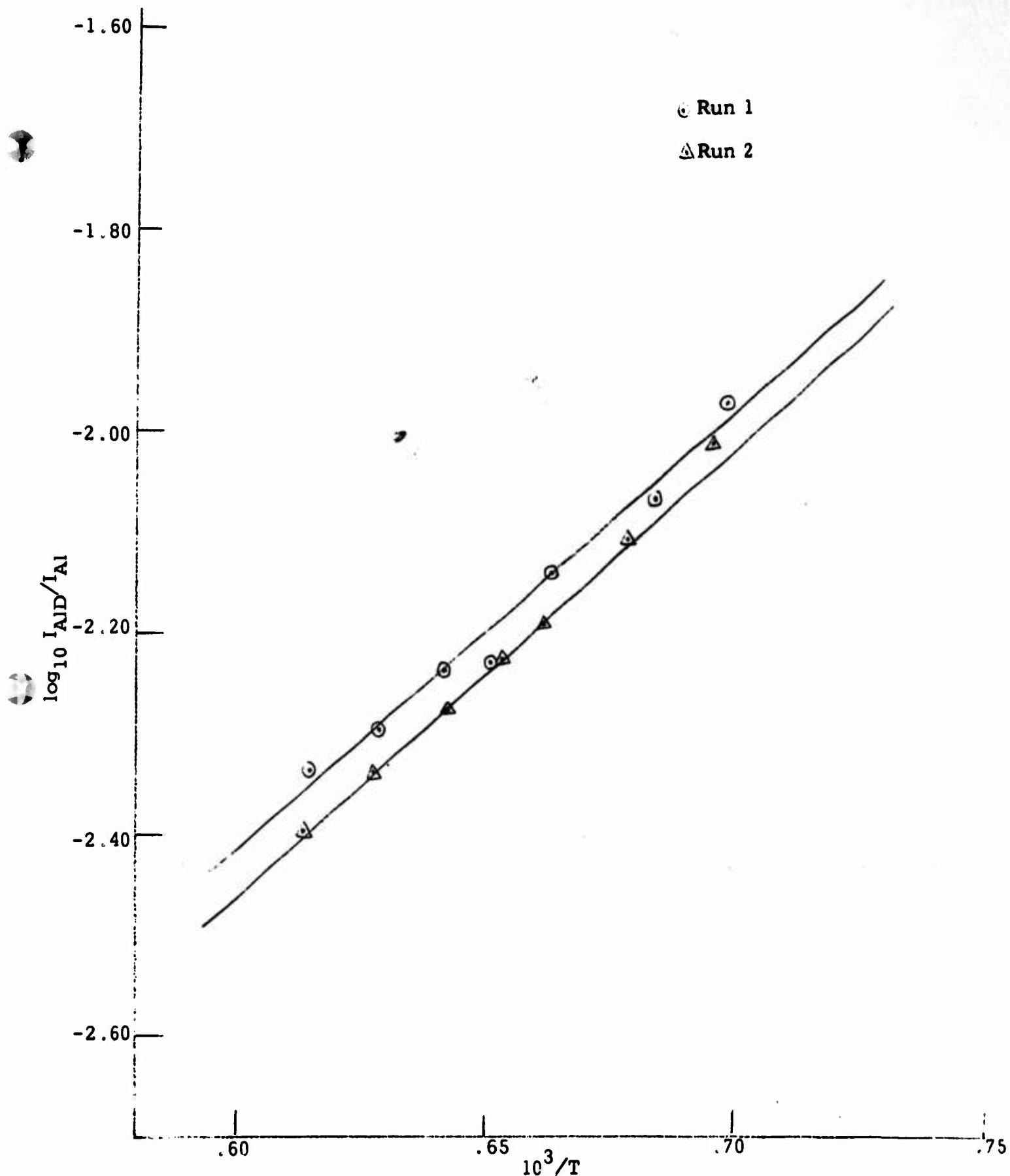


Fig. 4. Plot of $\log_{10} (I_{AID}/I_{AI})$ vs $1/T$ representing the reaction $Al(g) + 1/2D_2(g) = AlD(g)$, $D_2 = 10^{-4}$ atm (const.)

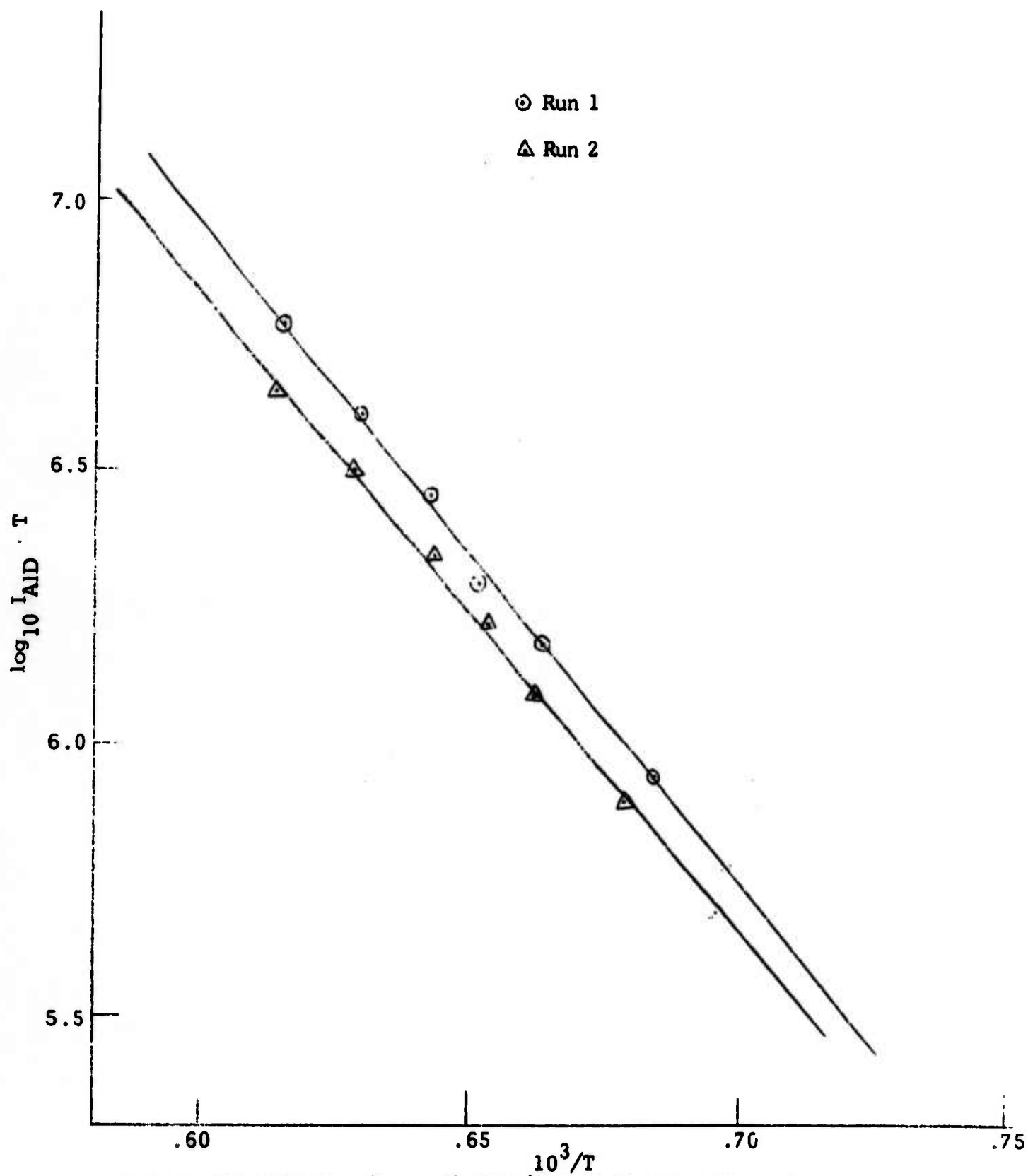


Fig. 5. Plot of $\log_{10} (I_{AID} \cdot T)$ vs $1/T$ representing the reaction
 $Al(l) + 1/2D_2(g) = AlD(g)$, $D_2 = 10^{-4}$ atm (const.)

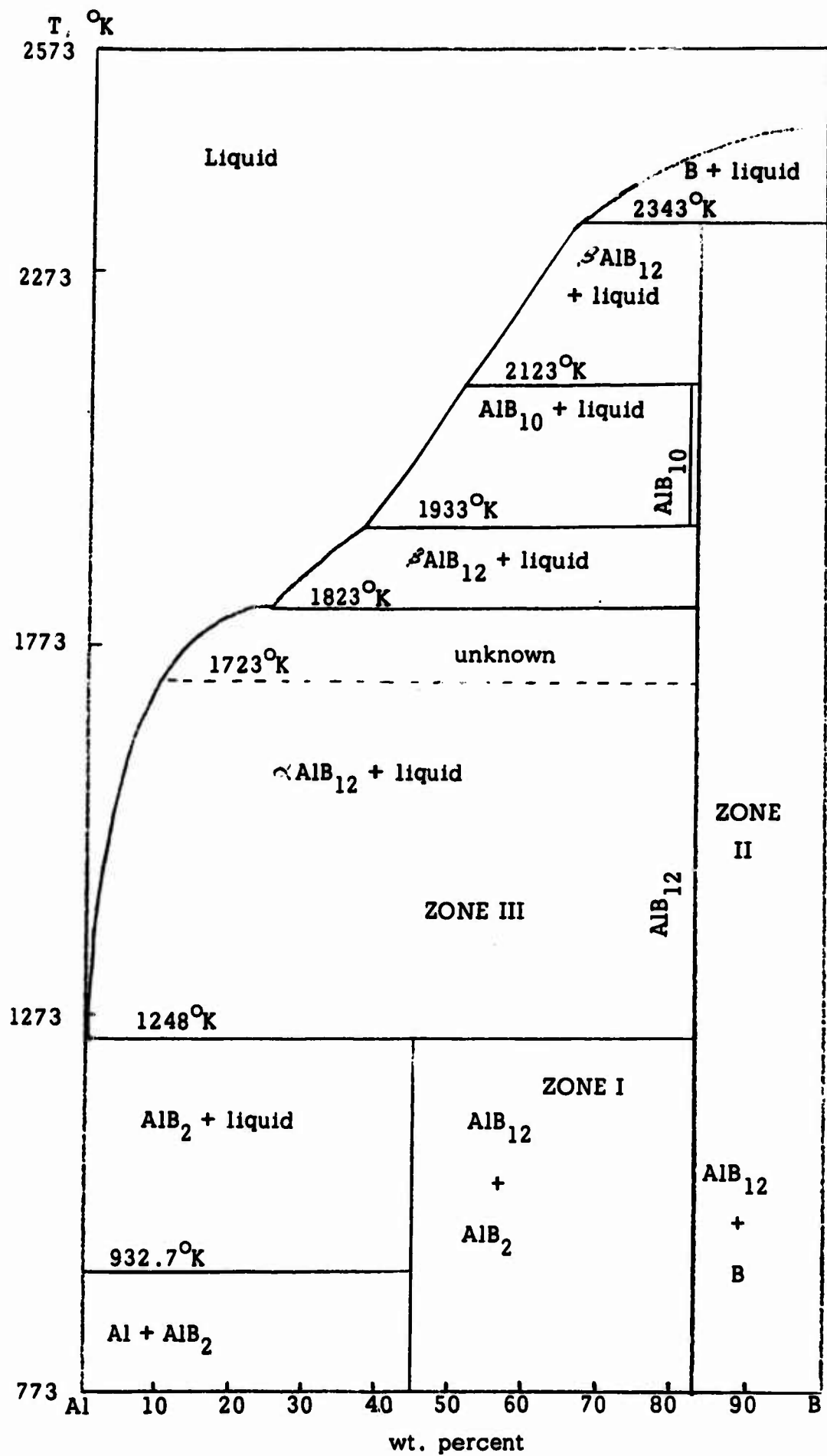


Fig. 6. Phase Diagram

Fig. 7. Plot of $\log_{10} (I_{Al} \cdot T)$ vs $1/T$ representing the reaction $\alpha \text{AlB}_{12}(c) = \text{Al}(g) + 12\text{B}(c)$

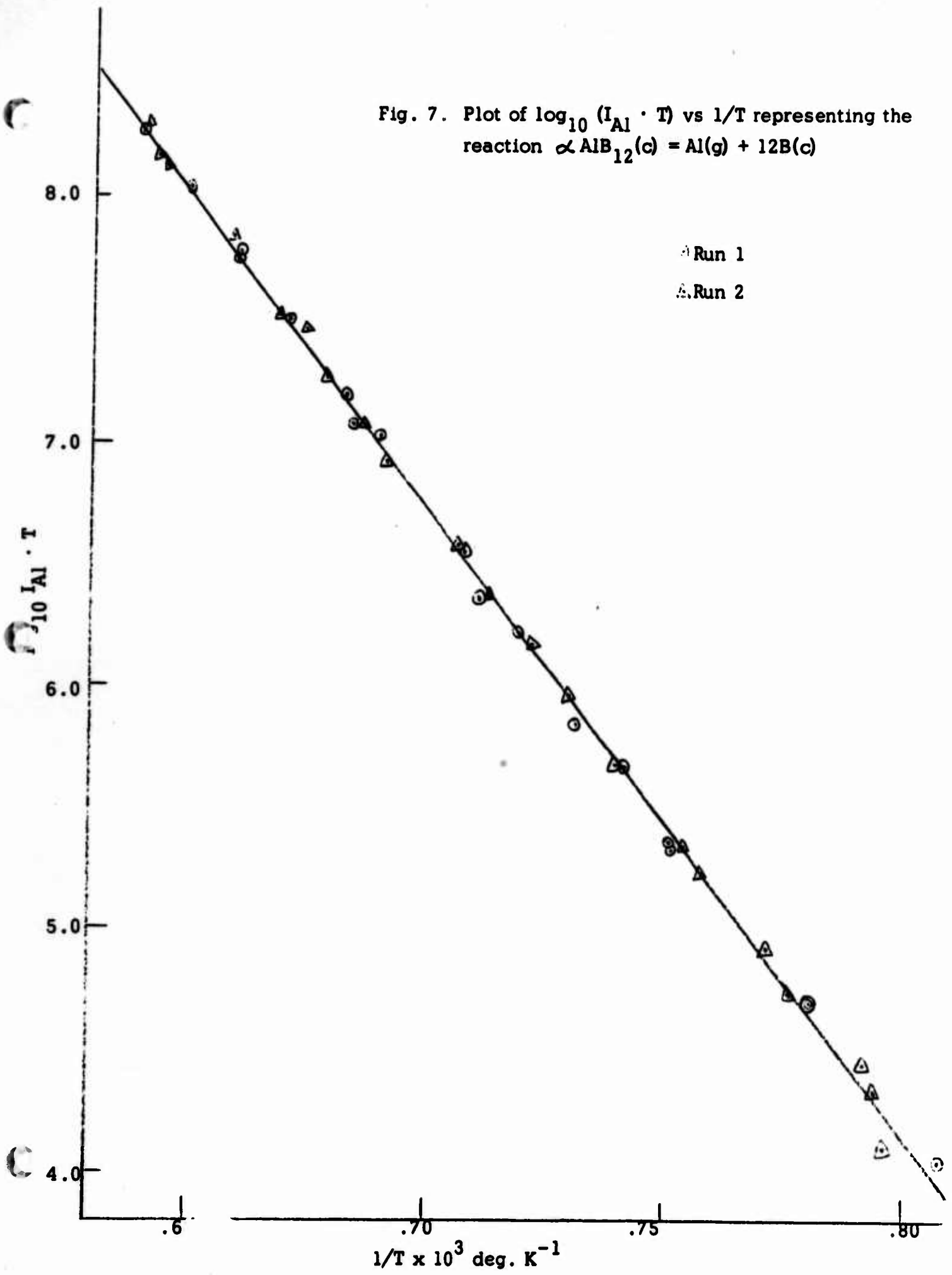
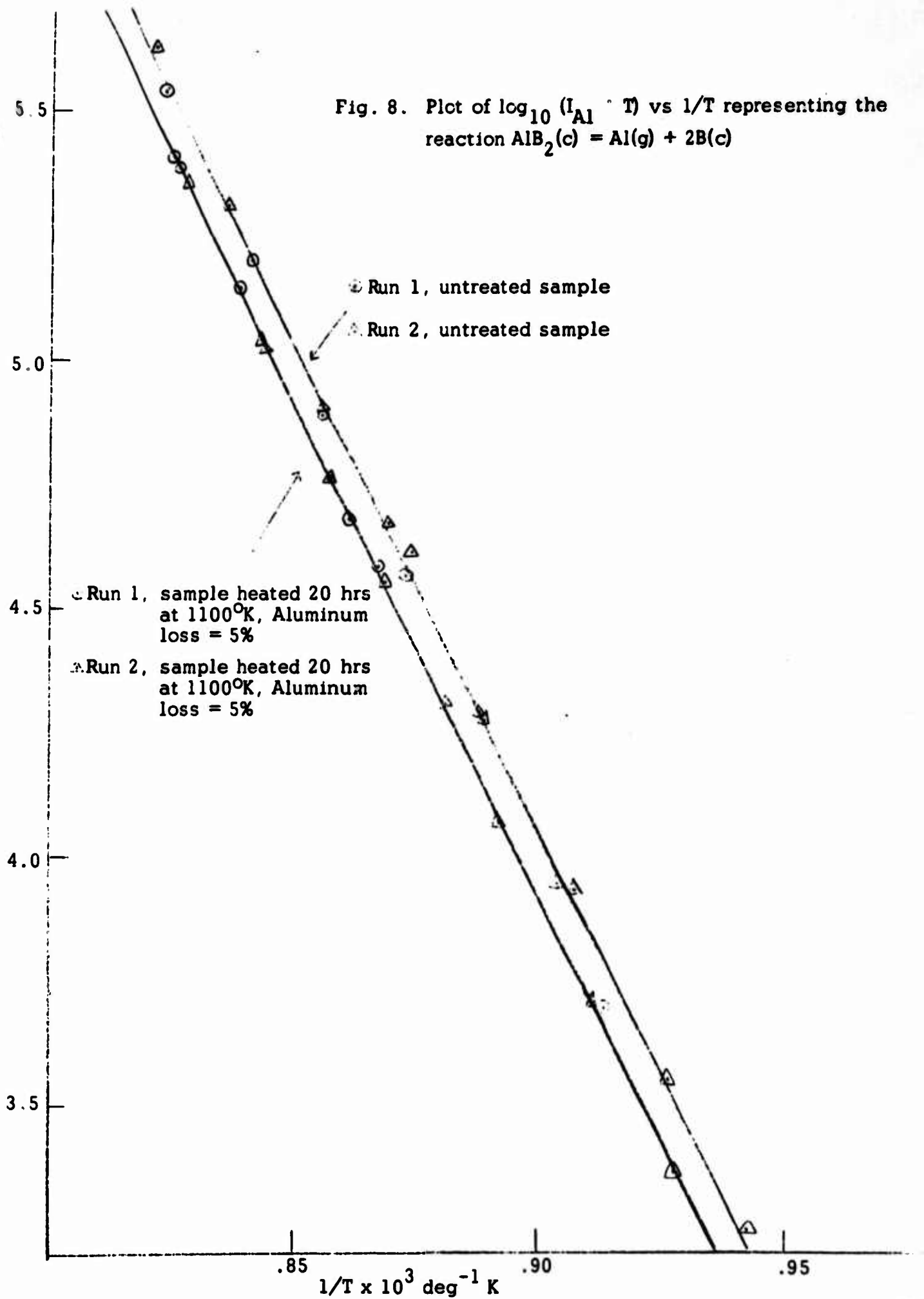


Fig. 8. Plot of $\log_{10} (I_{Al} \cdot T)$ vs $1/T$ representing the reaction $AlB_2(c) = Al(g) + 2B(c)$



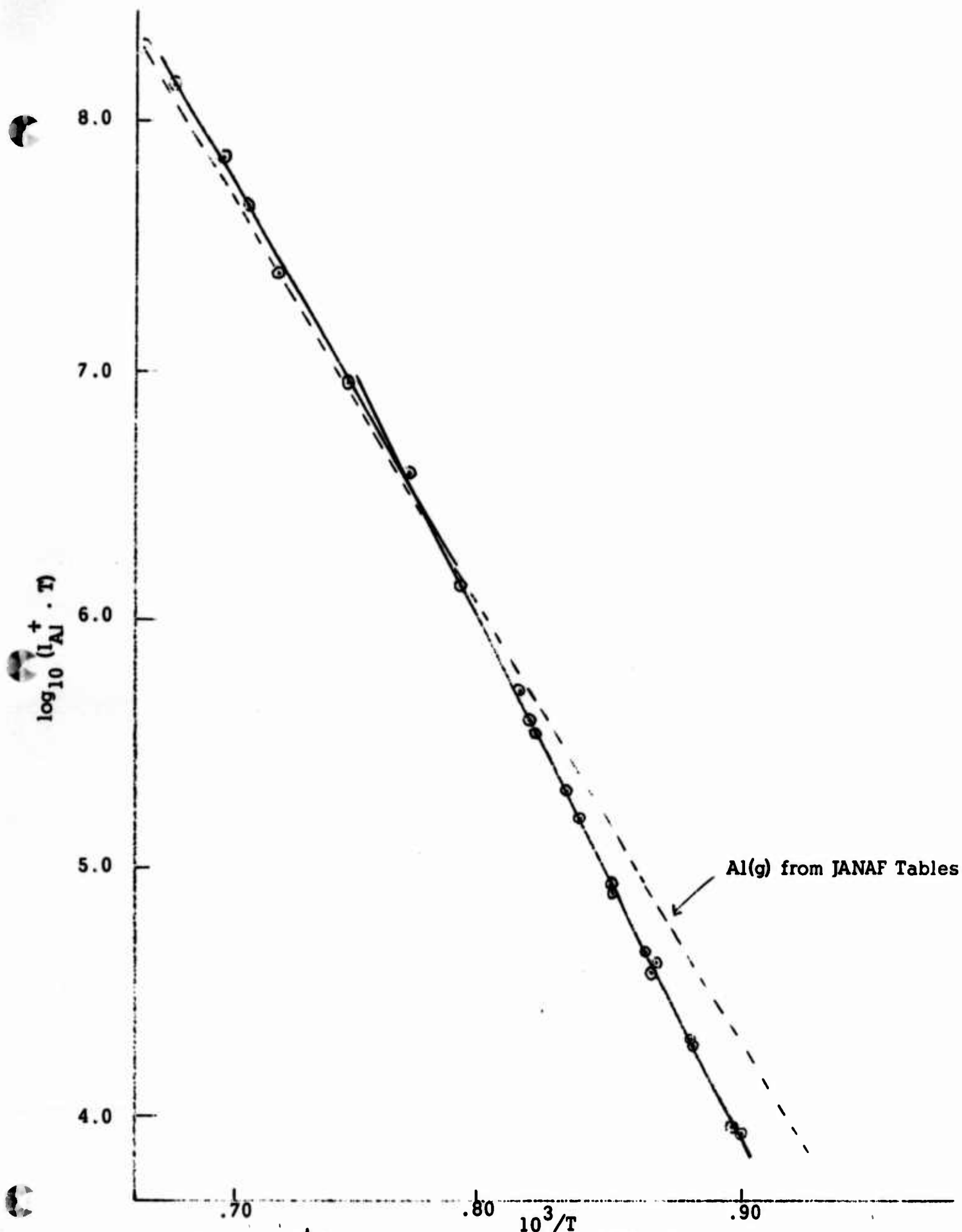


Fig. 9. Al^+ Intensities from a sample of $AlB_2(c)$ heated from $1060 - 1510^\circ K$

Unclassified
Security Classification

DOCUMENT CONTROL DATA - R&D

(Security classification of title, body of abstract and indexing annotation must be entered when the overall report is classified)

1. ORIGINATING ACTIVITY (Corporate author) Space Sciences, Inc.		2a. REPORT SECURITY CLASSIFICATION Unclassified	
		2b. GROUP	
3. REPORT TITLE Investigation of the Thermodynamic Properties of Rocket Combustion Products			
4. DESCRIPTIVE NOTES (Type of report and inclusive dates) Final Report, 30 October 1967 through 30 April 1968			
5. AUTHOR(S) (Last name, first name, initial) FARBER, Milton FRISCH, Margaret A.			
6. REPORT DATE June 1968		7a. TOTAL NO. OF PAGES 34	7b. NO. OF REFS 13
8a. CONTRACT OR GRANT NO. F04611-68-C-0020		8b. ORIGINATOR'S REPORT NUMBER(S)	
a. PROJECT NO. 3148			
b. BPSN: 623148		8c. OTHER REPORT NO(S) (Any other numbers that may be assigned to this report)	
c. Program El. Nr. 6.24.05.18.F			
10. AVAILABILITY/LIMITATION NOTICES This document is subject to special export controls and each transmittal to foreign governments or foreign nationals may be made only with the prior approval of AFRPL (RPPR-STINFO), Edwards, Calif. 93523.			
11. SUPPLEMENTARY NOTES		12. SPONSORING MILITARY ACTIVITY Department of the Air Force AFRPL (AFSC) Edwards, Calif. 93523	
13. ABSTRACT A research program has been conducted for the past six months involving molecular flow effusion and mass spectrometric techniques in which thermodynamic properties were obtained for: AlH(g) AlH ₂ (g) Al(g) \propto AlB ₁₂ (c) AlB ₂ (c)			

Unclassified

Security Classification

14. KEY WORDS	LINK A		LINK B		LINK C	
	ROLE	WT	ROLE	WT	ROLE	WT
Thermodynamic properties; heats of formation; entropies; exhaust species; light metal compounds; aluminum compounds; boron compounds.						

INSTRUCTIONS

1. **ORIGINATING ACTIVITY:** Enter the name and address of the contractor, subcontractor, grantee, Department of Defense activity or other organization (cooperate author) issuing the report.
- 2a. **REPORT SECURITY CLASSIFICATION:** Enter the overall security classification of the report. Indicate whether "Restricted Data" is included. Marking is to be in accordance with appropriate security regulations.
- 2b. **GROUP:** Automatic downgrading is specified in DoD Directive 5200.10 and Armed Forces Industrial Manual. Enter the group number. Also, when applicable, show that optional markings have been used for Group 3 and Group 4 as authorized.
3. **REPORT TITLE:** Enter the complete report title in all capital letters. Titles in all cases should be unclassified. If a meaningful title cannot be selected without classification, show title classification in all capitals in parenthesis immediately following the title.
4. **DESCRIPTIVE NOTES:** If appropriate, enter the type of report, e.g., interim, progress, summary, annual, or final. Give the inclusive dates when a specific reporting period is covered.
5. **AUTHOR(S):** Enter the name(s) of author(s) as shown on or in the report. Enter last name, first name, middle initial. If military, show rank and branch of service. The name of the principal author is an absolute minimum requirement.
6. **REPORT DATE:** Enter the date of the report as day, month, year, or month, year. If more than one date appears on the report, use date of publication.
- 7a. **TOTAL NUMBER OF PAGES:** The total page count should follow normal pagination procedures, i.e., enter the number of pages containing information.
- 7b. **NUMBER OF REFERENCES:** Enter the total number of references cited in the report.
- 8a. **CONTRACT OR GRANT NUMBER:** If appropriate, enter the applicable number of the contract or grant under which the report was written.
- 8b, 8c, & 8d. **PROJECT NUMBER:** Enter the appropriate military department identification, such as project number, subproject number, system numbers, task number, etc.
- 9a. **ORIGINATOR'S REPORT NUMBER(S):** Enter the official report number by which the document will be identified and controlled by the originating activity. This number must be unique to this report.
- 9b. **OTHER REPORT NUMBER(S):** If the report has been assigned any other report numbers (either by the originator or by the sponsor), also enter this number(s).
10. **AVAILABILITY/LIMITATION NOTICES:** Enter any limitations on further dissemination of the report, other than those

imposed by security classification, using standard statements such as:

- (1) "Qualified requesters may obtain copies of this report from DDC."
- (2) "Foreign announcement and dissemination of this report by DDC is not authorized."
- (3) "U. S. Government agencies may obtain copies of this report directly from DDC. Other qualified DDC users shall request through _____."
- (4) "U. S. military agencies may obtain copies of this report directly from DDC. Other qualified users shall request through _____."
- (5) "All distribution of this report is controlled. Qualified DDC users shall request through _____."

If the report has been furnished to the Office of Technical Services, Department of Commerce, for sale to the public, indicate this fact and enter the price, if known.

11. **SUPPLEMENTARY NOTE:** Use for additional explanatory notes.
12. **SPONSORING MILITARY ACTIVITY:** Enter the name of the departmental project office or laboratory sponsoring (paying for) the research and development. Include address.
13. **ABSTRACT:** Enter an abstract giving a brief and factual summary of the document indicative of the report, even though it may also appear elsewhere in the body of the technical report. If additional space is required, a continuation sheet shall be attached.

It is highly desirable that the abstract of classified reports be unclassified. Each paragraph of the abstract shall end with an indication of the military security classification of the information in the paragraph, represented as (TS), (S), (C), or (U).

There is no limitation on the length of the abstract. However, the suggested length is from 130 to 225 words.

14. **KEY WORDS:** Key words are technically meaningful terms or short phrases that characterize a report and may be used as index entries for cataloging the report. Key words must be selected so that no security classification is required. Identifiers, such as equipment model designation, trade name, military project code name, geographic location, may be used as key words but will be followed by an indication of technical context. The assignment of links, roles, and weights is optional.

Unclassified

Security Classification